Interrogation of Heme Pocket Environment of Mammalian Peroxidases with Diatomic Ligands†

Husam M. Abu-Soud*,‡ and Stanley L. Hazen*,§

Departments of Cell Biology and Cardiology and Center for Cardiovascular Diagnostics, Cleveland Clinic Foundation, Cleveland, Ohio 44195, and Chemistry Department, Cleveland State University, Cleveland, Ohio 44110

Received March 9, 2001; Revised Manuscript Received June 21, 2001

ABSTRACT: Recent studies demonstrate that myeloperoxidase (MPO), eosinophil peroxidase (EPO), and lactoperoxidase (LPO), homologous members of the mammalian peroxidase superfamily, can all serve as catalysts for generating nitric oxide- (nitrogen monoxide, NO) derived oxidants. These enzymes contain heme prosthetic groups that are ligated through a histidine nitrogen and use H_2O_2 as the electron acceptor in the catalysis of oxidative reactions. Here we show that heme reduction of these peroxidases results in distinct electronic and/or conformational changes in their heme pockets using a combination of rapid kinetics measurements, optical absorbance, and diatomic ligand binding studies. Addition of reducing agent to each peroxidase at ground state [Fe(III) state] causes immediate buildup of the corresponding Fe(II) complexes. Spectral changes indicate that two LPO−Fe(II) species are present in solution at equilibrium. Analyses of stopped-flow traces collected when EPO, MPO, or LPO solutions rapidly mixed with NO were accurately fit by single-exponential functions. Plots of the apparent rate constants as a function of NO concentration for all Fe(III) and Fe(II) forms were linear with positive intercepts, consistent with NO binding to each form in a simple reversible one-step mechanism. Fe(II) forms of MPO and LPO, but not EPO, displayed significantly lower affinity toward NO compared to Fe(III) forms, suggesting that heme reduction causes a dramatic change in the heme pocket electronic environment that alters the affinity and/or accessibility of heme iron toward NO. Optical absorbance spectra indicate that CO binds to the Fe(II) forms of both LPO and EPO, but not with MPO, and generates their respective low-spin six-coordinate complexes. Kinetic analyses indicate that the binding of CO to EPO is monophasic while CO binding to LPO is biphasic. Collectively, these results illustrate for the first time functional differences in the heme pocket environments of Fe(II) forms of EPO, LPO, and MPO toward binding of diatomic ligands. Our results suggest that, upon reduction, the heme pocket of MPO collapses, LPO adopts two spectroscopically and kinetically distinguishable forms (one partially open and the other relatively closed), and EPO remains open.

Myeloperoxidase (MPO),[1] eosinophil peroxidase (EPO), and lactoperoxidase (LPO) are homologous members of the mammalian peroxidase superfamily (*1, 2*). These heme-containing enzymes are products of distinct genes yet are structurally and functionally related (*1*−*5*). The enzymes have been characterized, and although they differ from each other with respect to their sites of expression, their primary sequences, and their substrate specificities, they are similar regarding catalysis and composition (*1*−*5*). For example, the three enzymes are heavily glycosylated and display the unique ability to catalyze the H_2O_2-dependent peroxidation of halides and pseudohalides to produce antimicrobial agents, hypohalous acids (*6*−*10*). Hypohalous acids are thought to play an important role in killing microorganisms; however, they also can injure normal tissues by bleaching the heme groups of hemoproteins and oxidatively destroying electron transport chains (*11, 12*). The reaction of peroxidases and the cosubstrate H_2O_2 likely involves oxygen transfer to Fe(III) to form active intermediates, compounds I and II, which can also generate cytotoxic oxidants and diffusible radical species (*13*−*18*). Compound I is a short-lived intermediate in the classic peroxidase cycle and readily is reduced 1 electron equiv, forming compound II, a longer-lived intermediate whose decay to ground state is considered to be the rate-limiting step during steady-state catalysis (*19, 20*). Enhancement in peroxidase catalysis due to reduction of compounds I and II have been noted with a series of organic substrates (*19*−*23*) and physiological reductants such as superoxide ($O_2^{\bullet -}$) (*19*), ascorbic acid (*24*), and nitric oxide (NO, nitrogen monoxide) (*25, 26*). NO, superoxide, and O_2 also can serve as ligands for Fe(III) and/or Fe(II) of peroxidases to generate either inactive nitrosyl or dioxy complexes (*19, 25*−*27*).

† This work was supported in part by National Institutes of Health Grants HL62526, HL61878 (S.L.H.), and HL66367 (H.M.A.-S.).

* Address correspondence to either author at the Department of Cell Biology, Lerner Research Institute, Cleveland Clinic Foundation, 9500 Euclid Ave., NC-10, Cleveland, OH 44195. Tel 216/445−9763; fax 216/444−9404; e-mail hazens@ccf.org or abusouh@ccf.org.

‡ Department of Cell Biology, Cleveland Clinic Foundation.

§ Cleveland Clinic Foundation and Cleveland State University.

[1] Abbreviations: Fe(III), ferric; Fe(II), ferrous; H_2O_2, hydrogen peroxide; k_{on}, association rate constant; k_{off}, dissociation rate constant; MPO, myeloperoxidase; EPO, eosinophil peroxidase; LPO, lactoperoxidase; NOS, nitric oxide synthase; NO, nitric oxide (nitrogen monoxide); CO, carbon monoxide.

10.1021/bi010478v CCC: $20.00
Published on Web 08/14/2001

MPO, an abundant hemoprotein present in neutrophils and monocytes, plays an essential role in immune surveillance and host defense mechanisms (*28*). The enzyme is a 150−165 kDa homodimer comprising two identical subunits joined by a single disulfide bridge (*29*). Each subunit is made up of a light chain and heavy chain derived from a single gene product (*29*, *30*). The heavy chains contain an iron bound by a novel protoporphyrin IX derivative, which is covalently linked to the heavy-chain polypeptide (*31*−*33*). Structural studies demonstrate that the heme of MPO lies at the base of a deep and narrow pocket and is less solvent-exposed compared to other peroxidases (*33*, *34*). The heme prosthetic groups are approximately 50 Å apart, appear functionally identical, and presumably operate independently in the oxidation of Cl^- and in the enzyme's bactericidal activity. EPO is a monomer comprising light and heavy chains with molecular masses of 50 and 15.5 kDa, respectively (*24*). This enzyme is stored in eosinophil granules and catalyzes the formation of antimicrobial species from the oxidation of Br^- and SCN^- (*24*, *35*−*36*). LPO is a monomeric single-chain polypeptide of molecular mass 78.5 kDa (*37*−*40*). LPO is believed to play an important role in antimicrobial defenses within exocrine gland secretions such as milk, saliva, and tears (*41*, *42*). The amino acid sequences of the three peroxidases are known and show that they share 50−70% overall homology (*5*). MPO is the only member of this family for which the X-ray-derived structure is presently available (*33*, *34*). However, a theoretical three-dimensional model for LPO and EPO built on the scaffold of the MPO X-ray structure suggested that the enzymes share the same general structural features (*43*).

The reaction of NO with the metal centers of hemoproteins at nearly diffusion-controlled rates is well-known and mediates activation of guanylate cyclase as well as inhibition of many proteins (*44*−*51*). For example, NO and NO releasing agents have been implicated in inhibition of cytochrome P450 via the formation of an iron−nitrosyl complex that prevents access of O_2 to the catalytic site of the enzyme (*46*). NO also mediates inhibition of mitochondrial cytochrome *c* oxidase and deenergizes mitochondria at low NO and O_2 concentrations (*48*). Recent studies from our lab demonstrated that NO modulates the catalytic activity of MPO by distinct mechanisms. NO accelerates both the formation and decay of compound II, the rate-limiting step in the classic peroxidase cycle (*25*, *26*). At higher levels of NO, reversible inhibition of MPO occurs through the formation of MPO−Fe(III)−NO complex (*25*, *26*). Thus, NO serves as both a ligand and a substrate for MPO, and the overall effect of NO on the catalytic activity depends on the affinity of MPO for NO vs H_2O_2 and their concentrations (*25*, *26*).

We recently demonstrated that NO binds to both ferric and ferrous forms of MPO, generating stable low-spin six-coordinate nitrosyl complexes (*25*). The rate of NO binding to ferrous MPO was slowed considerably with respect to ferric form, indicating that heme reduction limits the affinity of NO for the heme iron. This behavior is not typical for hemoproteins (*52*−*56*) and suggests that reduction of MPO−Fe(III) induces unusual structural (i.e., collapse or narrowing) and/or electronic alterations in the heme pocket (*25*). Whether similar behavior is observed with other members of the mammalian peroxidase superfamily is not known. In the present studies we utilize a combination of optical absorbance, rapid kinetics measurements, and diatomic ligand binding studies to assess the distinct conformational changes that occur upon reduction in the heme pocket geometry of EPO and LPO compared to MPO. Our results indicate that heme reductions of EPO, LPO, and MPO have different effects on the heme iron environment and suggest that conformational and/or electronic changes associated with heme reduction differentially affect the affinity of the heme group of mammalian heme peroxidases for diatomic ligands.

MATERIALS AND METHODS

Materials. NO and CO gases were purchased from Matheson Gas Products, Inc., and used without further purification. All other reagents and materials were of the highest purity grades available and obtained from either Sigma Chemical Co. or Aldrich.

Enzyme Purification. EPO was purified from porcine whole blood as previously described (*57*). The purity of EPO was confirmed by demonstrating an RZ of >1.00 (A_{415}/A_{280}), SDS−PAGE analysis with Coomassie blue staining, and in-gel tetramethylbenzidine peroxidase staining. MPO was purified from detergent extracts of human leukocytes as described (*58*). Trace levels of contaminating EPO were then removed by passage over a sulfopropyl-Sephadex column (*59*). Purity of isolated MPO was established by demonstrating an RZ of >0.85 (A_{430}/A_{280}), SDS−PAGE analysis with Coomassie Blue staining, and in-gel tetramethylbenzidine peroxidase staining to confirm no contaminating EPO activity (*57*). Enzyme concentrations were determined spectrophotometrically utilizing extinction coefficients of 89 000 and 112 000 M^{-1} cm^{-1}/heme of MPO (*60*) and EPO (*24*, *61*), respectively. LPO was obtained from Worthington Biochemical Corp. (Lakewood, NJ) and used without further purification. Purity was confirmed by demonstrating an RZ of 0.75 (A_{412}/A_{280}) and SDS−PAGE analysis with Coomassie Blue staining.

Optical Spectroscopy and Rapid Kinetic Measurements. Optical spectra were recorded on either a Perkin-Elmer (Lambda Bio) or Hitachi 3010 UV−visible spectrophotometer at 25 °C. Anaerobic spectra were recorded by use of septum-sealed quartz cuvettes that could be attached through a quick-fit joint to an all-glass vacuum system. EPO, LPO, or MPO samples were made anaerobic by several cycles of evacuation and equilibrated with catalyst-deoxygenated N_2. Separate buffer solutions were evacuated, gassed with N_2, and anaerobically transferred either to the stopped-flow instrument or to anaerobic cuvettes with gastight syringes. Cuvettes were maintained under N_2, CO, or NO positive pressure during spectral measurements. All kinetic measurements were performed with a temperature-controlled stopped-flow apparatus (Hi-Tech, model SF-51) equipped for efficient anaerobic work. Measurements were carried out at 10 °C and initiated by rapidly mixing equal volumes of the enzyme solutions (0.86 μM) with buffer solution supplemented with increasing concentrations of NO or CO. The reactions for CO and NO binding to the three enzymes were monitored at wavelengths determined from the spectral changes that occur upon CO or NO binding to the Fe(II) and Fe(III) forms of the enzymes, as indicated. To determine the apparent rate constants for the formation of Fe(III)−NO, Fe(II)−NO, and Fe(II)−CO complexes, the time course of absorbance change

was fit to either single- ($Y = 1 - e^{-kt}$) or double- ($Y = Ae^{-k_1 t} + Be^{-k_2 t}$) exponential functions as indicated, by use of a nonlinear least-squares method provided by the instrument manufacturer. Signal-to-noise ratios were improved by averaging 7−10 individual traces.

Solution Preparation. A fresh saturated stock of CO or NO was prepared under strict anaerobic conditions. For NO solution, the extent of nitrite/nitrate (NO_2^-/NO_3^-) build-up in NO preparations over the time of use for the present studies was <1−1.5%/mol of NO, as determined by anion-exchange HPLC (*26, 62*), under anaerobic conditions. Anaerobic 0.2 M sodium phosphate buffer solutions, pH 7.0, containing various concentrations of NO or CO were prepared by mixing different volumes of buffer saturated with NO or CO gas at 21 °C with anaerobic buffer solution. Saturating concentration of CO and NO at 21 °C is approximately 1 and 2 mM, respectively.

RESULTS

Formation, Stability, and Reversibility of Fe(III)−NO and Fe(II)−NO Complexes for EPO and LPO. Spectroscopic studies demonstrated that addition of NO to EPO−Fe(III) caused immediate nitrosyl complex formation, as judged by a decrease and shift in the Soret absorbance peak from 413 to 426 nm, and the appearance of additional absorbance peaks in the visible range at 547 and 588 nm (Figure 1A, Table 1). Addition of a slight molar excess of dithionite to EPO−Fe(III) caused a disappearance of the Soret band at 413 nm and the appearance of a new band at 450 nm, indicating that EPO heme iron is reduced. The EPO−Fe(II) complex was stable under anaerobic atmosphere and EPO−Fe(III) was completely recovered after exposure of EPO−Fe(II) to air. Addition of NO to EPO−Fe(II) caused a shift in Soret absorbance from 450 to 436 nm and an increase and shift in the visible bands at 547 and 590 nm (Figure 1B, Table 1), indicating the formation of an EPO−Fe(II)-NO complex. The insets of Figure 1 show the difference spectra of the Fe(III) and Fe(II) forms of EPO against their respective nitrosyl complexes. Collectively, these results indicate that NO binds to both ferric and ferrous forms of EPO to generate low-spin six-coordinate Fe(III)−NO and Fe(II)−NO complexes, respectively. In both cases, no further spectral changes were observed after 30 min under anaerobic conditions, indicating that the EPO−nitrosyl complexes are stable. The original spectra were restored by removal of NO under anaerobic conditions, indicating the reversible nature of these complexes.

Spectroscopic studies demonstrate that LPO−Fe(III) displays a Soret absorbance peak at 413 nm and additional visible peaks at 502, 544, and 635 nm. Addition of a slight molar excess of dithionite to the enzyme solution caused immediate buildup of a LPO−Fe(II) complex that displayed a Soret maximum centered at 447 nm. However, this species was unstable because the Soret maximum gradually shifted to 433 nm within minutes (Figure 2B). This spectral change indicates that at least two LPO−Fe(II) species are present in the solution at equilibrium (Figure 2B, inset). Addition of NO to LPO−Fe(III) solution caused an immediate buildup of an Fe(III)−NO complex characterized by a Soret maximum at 417 nm (Figure 2A). As shown in Figure 2A, addition of a slight molar excess of dithionite to the LPO−

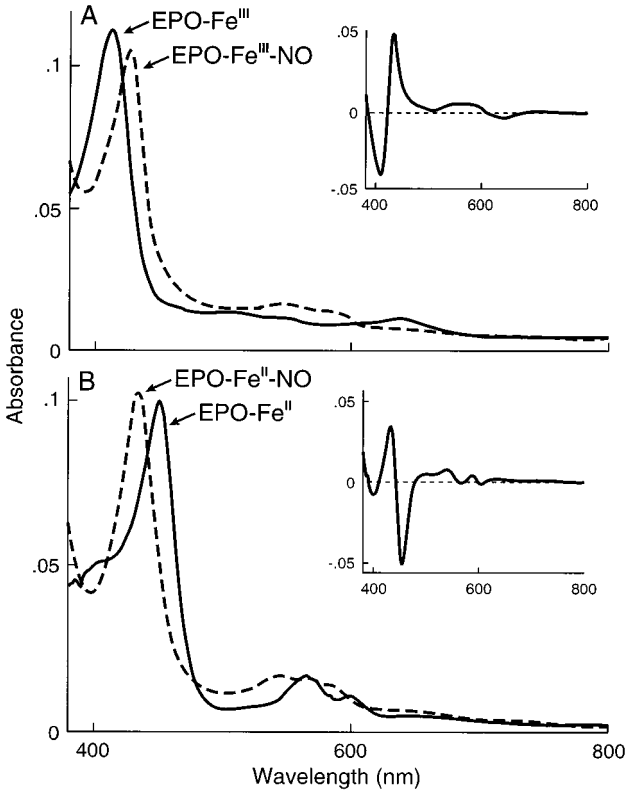

FIGURE 1: Spectral changes upon NO binding to EPO ferric and ferrous forms. (A) Absorbance spectra of EPO−Fe(III) before (—) and after (---) the addition of NO. (B) Absorbance spectra of EPO−Fe(II) before (—) and after (---) the addition of NO. The spectrum of EPO−Fe(II) was obtained by reduction of EPO−Fe(III) with a slight molar excess of sodium dithionite. Experiments were performed under anaerobic conditions in sodium phosphate buffer (200 mM, pH 7.0) containing 0.86 μM EPO in the absence and presence of 300 μM NO at 25 °C. Difference spectra were generated by subtracting the spectrum of EPO−Fe(III)−NO from that of native enzyme (inset, panel A) or the spectrum of EPO−Fe(II)−NO from that of EPO−Fe(II) (inset, panel B).

Fe(III)−NO complex produced a spectrum consistent with formation of a low-spin six-coordinate LPO−Fe(II)−NO complex. This complex displays a Soret absorbance peak at 423 nm and additional visible peaks at 545 and 582 nm. Alternatively, adding NO to prereduced LPO (Figure 2B) also generated the LPO−Fe(II)−NO complex. In all cases the LPO−nitrosyl complexes were stable and the original spectra were recovered by degassing NO under anaerobic atmosphere. Together, the prominent spectral features in the Soret and visible regions for Fe(III) and Fe(II) forms of EPO, LPO, and their respective nitrosyl complexes, along with that previously reported for MPO (*25*), are summarized in Table 1.

Stopped-Flow Analysis of NO Binding to EPO and LPO. To compare the perturbations in the heme pocket environment of MPO (*25*), EPO, and LPO that occur upon heme reduction, and to assess the potential physiological relevance of NO to the three enzymes, we extended our investigation to examine rates of NO binding to ferric and ferrous forms of EPO and LPO heme iron. Rapid kinetic measurements were performed under anaerobic conditions to determine the combination (k_{on}) and dissociation (k_{off}) rates of NO binding to both Fe(III) and Fe(II) forms of EPO and LPO under conditions similar to those recently reported for MPO (*25*). Experiments were carried out under pseudo-first-order condi-

Table 1: Spectroscopic and Kinetic Characterization of NO and CO Binding to Ferrous and Ferric (NO Only) Forms of EPO, LPO, and MPO[a]

complex	Soret (nm)	visible bands (nm)	k_{on} (M^{-1} s^{-1})	k_{off} (s^{-1})
EPO−Fe(III)	413	507, 550, 640		
EPO−Fe(II)	450	566, 600		
EPO−Fe(III) + NO	426	547, 588	1.35×10^6	65
EPO−Fe(II) + NO	436	547, 590	1.29×10^6	24
EPO−Fe(II) + CO	436	550, 587	0.65×10^3	0.012
LPO−Fe(III)	413	502, 544, 635		
LPO−Fe(II) (immediate)	447	563, 598		
LPO−Fe(II) (final)	433	563, 598		
LPO−Fe(III) + NO	417	542, 577	$>3.00 \times 10^6$	b
LPO−Fe(II) + NO	423	545, 582	1.40×10^5	0.25
LPO−Fe(II) + CO	425	542, 577	0.59×10^3	0.0013
			1.40×10^3	0.029
MPO−Fe(III)	430	573, 630, 694		
MPO−Fe(II)	476	642		
MPO−Fe(III) + NO	433	575, 630	1.07×10^6	10.8
MPO−Fe(II) + NO	467	635	1.00×10^5	4.6
MPO−Fe(II) + CO	476	642		

[a] Absorbance maxima were obtained from Figures 1, 2, and 5. The interaction of NO and CO with the ferric (NO only) or ferrous forms of peroxidases were studied at 10 °C. The k_{on} and k_{off} rates were derived from the slope and intercept, respectively, following linear regression analysis of k_{obs} versus NO or CO concentration. [b] Not detected.

tions by rapid mixing of a prereduced or native enzyme with buffer solutions supplemented with different NO concentrations. In both cases, analysis of stopped-flow traces collected when EPO solutions rapidly mixed with NO was accurately fit by a single-exponential function. As shown in Figure 3, the plots of the apparent rate constants as a function of NO concentration for both EPO−Fe(III) and EPO−Fe(II) were linear, consistent with NO binding to each form in a simple one-step mechanism where $k_{obs} = k_{on}[NO] + k_{off}$. The positive intercepts confirm that NO bound to both EPO−Fe(III) and EPO−Fe(II) in a reversible manner.

Parallel studies examining NO interaction with LPO indicate that NO binds to LPO−Fe(III) faster than the instrument limits (2 ms dead time for acquisition) under the conditions employed. Although a rate constant for the combination of NO and LPO−Fe(III) could not be obtained at 10 °C, binding of NO to LPO−Fe(II) to form the respective Fe(II)−NO complex could be monitored by following the increase in absorbance at 423 nm. The plot of k_{obs} vs NO concentration was linear with *y*-intercept close to zero, indicating that the dissociation of NO from LPO−Fe(II)−NO is extremely slow (Figure 4). Together, the kinetic parameters obtained for NO binding to LPO along with EPO and MPO are summarized in Table 1.

Formation, Stability, and Reversibility of EPO−, LPO−, and MPO−Fe(II)−CO Complexes. Optical studies demonstrated that addition of CO to the reduced form of EPO produced an increase and a shift in the Soret absorbance peak from 450 to 436 nm, as well as additional absorbance peaks in the visible range at 550 and 587 nm (Figure 5 and Table 1). These results indicate that CO binds to EPO to form a six-coordinate low-spin Fe(II)−CO complex. The EPO−Fe(II)−CO complex is stable; however, the original spectrum was restored by degassing CO under anaerobic conditions, indicating the reversible nature of this complex. Similar results were obtained for LPO (Figure 5).

We also investigate the effect of CO on the optical spectrum of MPO−Fe(II), to compare the effect of MPO,

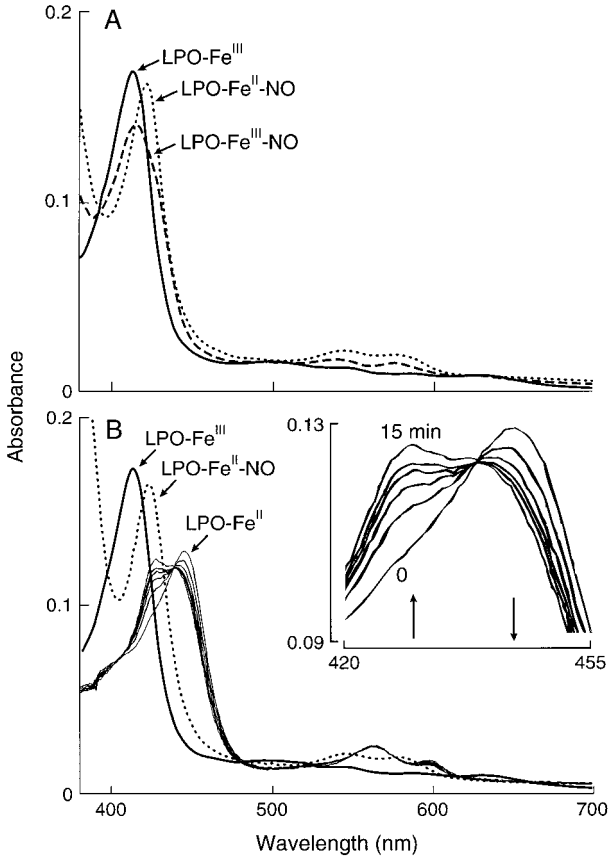

FIGURE 2: Spectral changes upon LPO heme reduction and NO binding to LPO ferric and ferrous forms. Panel A shows absorbance spectra for LPO−Fe(III) as isolated (ground state) (—), after addition of NO to form a LPO−Fe(III)−NO complex (---), and after reduction by dithionite to form the Fe(II)−NO complex (▪▪▪). Panel B shows the absorbance spectra for the enzyme as isolated [Fe(III) form] and after addition of a slight molar excess of sodium dithionite. Spectral traces were recorded immediately after reduction and then after every 3 min for up to 30 min. Addition of NO to LPO−Fe(II) at any time following heme reduction generates the same spectrum characteristic of LPO−Fe(II)−NO complex (▪▪▪). The inset of panel B magnifies the spectral changes that occur in the Soret region from 420 to 455 nm following heme reduction. Arrows in the inset indicate the direction of spectral change over time. Selected spectra were omitted from the panel for clarity. Experiments were carried out under anaerobic conditions in sodium phosphate buffer (200 mM, pH 7.0), at 25 °C.

EPO, and LPO heme reduction on their catalytic sites. MPO−Fe(II) displays a Soret absorbance peak at 476 nm and an additional visible peak at 642 nm, which were used to monitor CO binding. Unlike EPO, addition of CO to MPO−Fe(II) complex caused minimal changes in the Soret region, indicating that CO did not bind to MPO heme iron (Figure 5). These findings are consistent with MPO heme reduction causing alterations in the heme environment that limit interaction of CO with MPO heme iron (*25*, *63*).

Stopped-Flow Analysis of CO Binding to EPO and LPO. To examine how EPO and LPO heme reduction affects CO binding, we used stopped-flow spectroscopy and the kinetic parameters obtained were compared to rates of CO interaction with other hemoprotein model compounds. Kinetic analysis indicated that the buildup of EPO−Fe(II)−CO complex follows a monophasic reaction, and the plot of CO concentration vs observed rate was linear with positive *y*-intercept (Figure 6). These results indicate that CO binding to EPO−Fe(II) is reversible and follows a simple one-step

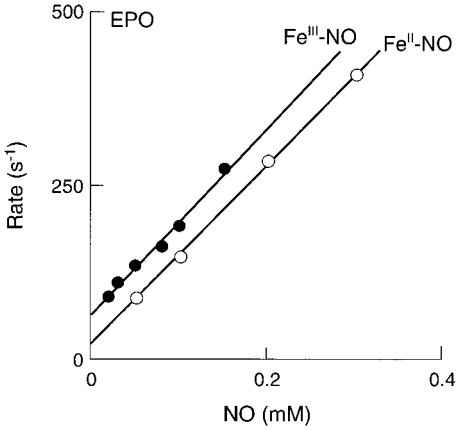

FIGURE 3: Plot of the observed rates of NO binding to EPO−Fe(III) and EPO−Fe(II) as a function of NO concentration. An anaerobic solution containing 0.86 μM EPO−Fe(II) was rapidly mixed with an equal volume of sodium phosphate buffer (200 mM, pH 7.0) supplemented with differing concentrations of NO at 10 °C. The observed rate of EPO−Fe(III)−NO (●) and EPO−Fe(II)−NO (○) formation were plotted as a function of NO concentration. The formation of EPO−Fe(III)−NO and EPO−Fe(II)−NO complexes were monitored at 413 and 460 nm, respectively.

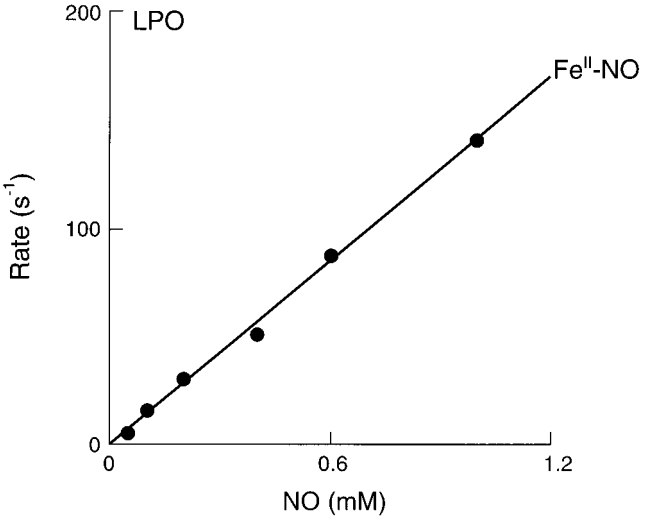

FIGURE 4: Plot of the observed rate of NO binding to LPO−Fe(II) as a function of NO concentration. An anaerobic solution containing 0.86 μM LPO−Fe(II) (>30 min following reduction) was rapidly mixed with an equal volume of sodium phosphate buffer (200 mM, pH 7.0) supplemented with differing concentrations of NO at 10 °C, and the buildup of Fe(II)−NO complex was monitored at 427 nm. The observed rates of EPO−Fe(II)−NO formation were plotted as a function of NO concentration.

mechanism where $k_{obs} = k_{on}[CO] + k_{off}$. The combination ($k_{on}$) and dissociation ($k_{off}$) rate constants calculated from the slope and intercept, respectively, are summarized in Table 1. Binding of the LPO−Fe(II)−CO complex was biphasic and best fit to two-exponential functions, indicating that at least two species are present. Between 50% and 60% was associated with the slow phase. Figure 7 shows the rate of the spectral changes for both the slow and fast phases as a function of CO concentration. In both cases, the plots were linear with finite positive intercepts at the *y*-axis, indicating that CO binding is reversible and follows a simple one-step mechanism (Figure 7). The k_{on} and k_{off} values derived from the graphs are summarized in Table 1.

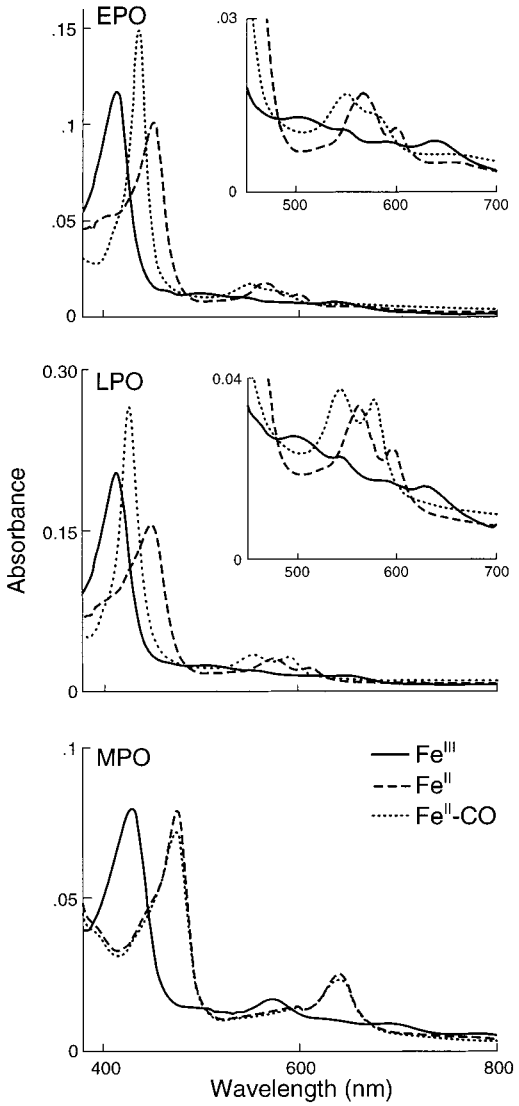

FIGURE 5: Spectral changes upon CO binding to EPO, LPO, and MPO ferrous forms. (Upper panel) UV/vis spectra show EPO−Fe(III) (—), after reduction by dithionite to form EPO−Fe(II) (---), and after addition of CO to form EPO−Fe(II)−CO (•••). The inset magnifies the three spectra in the region from 450 to 700 nm. (Middle panel) UV/vis spectra of LPO−Fe(III) (—), immediately after reduction by dithionite to form LPO−Fe(II) (---), and after addition of CO to form LPO−Fe(II)−CO (•••). The inset magnifies the three spectra in the region from 450 to 700 nm. (Lower panel) UV/vis spectra of MPO−Fe(III) (—), after reduction with dithionite to form MPO−Fe(II) (---), and after addition of CO to form MPO−Fe(II)−CO (•••). Experiments were performed under anaerobic conditions in sodium phosphate buffer (200 mM, pH 7.0) containing 0.86−1.5 μM EPO, LPO, or MPO in the absence and presence of 300 μM CO at 25 °C.

DISCUSSION

Members of the mammalian peroxidase superfamily, such as MPO, EPO, and LPO, are receiving increased attention because of their roles in host defenses and their potential contribution to the pathogenesis of tissue injury in inflammatory diseases (*21*, *64*−*69*). At ground state, these enzymes operate in their ferric forms to utilize H_2O_2 in the production of reactive oxidants and diffusible radical species. Although they utilize similar catalytic mechanisms, these distinct gene products demonstrate unique substrate selectivities and operate in distinct physiological environments. A variety of spectroscopic techniques including resonance Raman, elec-

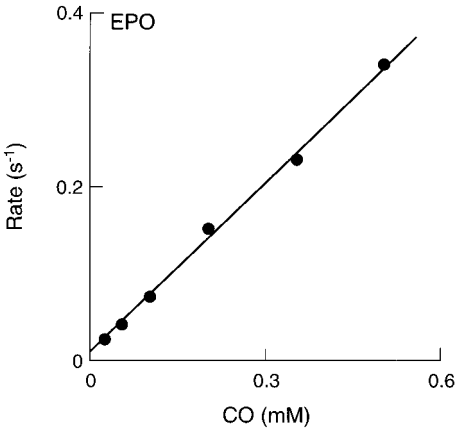

FIGURE 6: Plot of the observed rate of CO binding to EPO−Fe(II) as a function of CO concentration. An anaerobic solution containing 0.86 μM EPO−Fe(II) was rapidly mixed with an equal volume of sodium phosphate buffer (200 mM, pH 7.0) supplemented with differing concentrations of CO at 10 °C, and the buildup of Fe(II)−CO complex was monitored at 427 nm. The observed rates of EPO−Fe(II)−CO formation were plotted as a function of CO concentration.

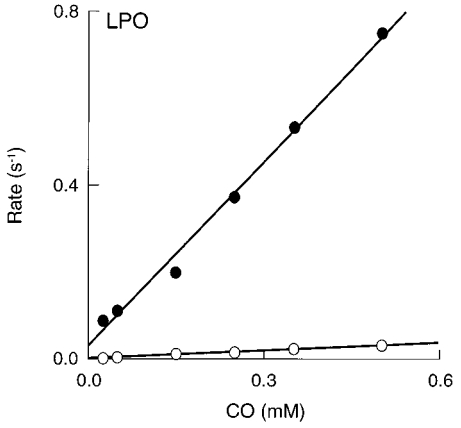

FIGURE 7: Plot of the observed rate of CO binding to LPO−Fe(II) as a function of CO concentration. An anaerobic solution containing 0.86 μM LPO−Fe(II) [prepared by mixing LPO−Fe(III) with a slight molar excess of dithionite 30 min earlier] was rapidly mixed with an equal volume of sodium phosphate buffer (200 mM, pH 7.0) supplemented with differing concentrations of CO, at 10 °C. Experiments were carried out by following the increase in absorbance at 425 nm. Spectral changes were best fit to two exponential functions. A plot of each of the observed rates of LPO−Fe(II)−CO formation as a function of CO concentration is shown. The two lines present in the figure indicate that CO binding under this condition was biphasic and each step follows a simple one-step mechanism.

tron paramagnetic resonance (EPR), magnetic circular dichroism, and X-ray structure indicate that the native enzymes exist primarily as hexacoordinate high-spin complexes with a water molecule or carboxylate amino acid residue present as a weak distal ligand (*33*, *34*, *70*−*73*). In the present studies we directly compare the ferric and ferrous forms of EPO, LPO, and MPO using diatomic ligands to interrogate the heme environment. The present results demonstrate that MPO, EPO, and LPO differentially ligate diatomic ligands and respond to heme reduction, processes that significantly reshape their catalytic sites, and in some cases are known to lead to inhibition of peroxidase activity (*19*).

On the basis of the present results and prior published studies (*31*−*34*, *43*, *73*−*77*), we have generated the following model of how mammalian peroxidases interact with diatomic ligands in the ferric and ferrous forms (Figure 8). NO binds reversibly to Fe(III) forms of EPO, LPO (this study), and MPO (*25*), through a simple one-step mechanism generating their respective low-spin six-coordinate Fe(III)−nitrosyl complexes. Nitrosyl complex formation was demonstrated for each peroxidase by direct spectroscopic techniques. Rapid kinetic methods demonstrated that the rates of NO interactions with ferric EPO are comparable to those observed with MPO (*25*) and other hemoproteins, while the rates of NO interactions with LPO−Fe(III) are faster than the detection limit of the stopped-flow apparatus under the conditions employed (Table 1). The rate constants for NO dissociation from ferric EPO− and MPO−nitrosyl complexes are relatively high compared to other hemoproteins, such as cytochrome *c*, hemoglobin, and microperoxidase, whose dissociation rate constants range from 0.03 to 3.4 s^{-1} (*51*, *55*, *79*). The high off rates observed with EPO and MPO are similar to the rates recently reported for iNOS, eNOS (*53*, *78*), and myoglobin (*51*, *55*). In contrast, the rate of NO dissociation from the LPO−Fe(III)−NO complex appears to be exceedingly slow. While we are unable to determine kinetic parameters for NO interaction with LPO−Fe(III) based upon the present studies, analysis of the interactions of NO with LPO intermediates during steady-state catalysis reveal a dominant role for NO-dependent sequestration of LPO into the LPO−Fe(III)−NO form, removing enzyme available for catalysis (Abu-Soud and Hazen, manuscript in preparation). The ability of ferric EPO, LPO, and MPO to bind NO with relatively high rates compared to other hemoproteins supports the hypothesis that their heme pockets are relatively open and readily accommodate NO as a sixth axial ligand (Figure 8).

Ferric hemoproteins may be reduced to ferrous forms by a variety of potential reductants. While the relevant reducing species for peroxidases in vivo are unclear, NADPH, ascorbate, and superoxide may play a role since they are been shown to serve as reductants for MPO and other ferric hemoproteins (*19*, *27*). In addition, ferric forms of peroxidases can bind superoxide to generate compound III, a ferrous−dioxy complex (*19*, *27*). This may dissociate to generate O_2 and ferrous forms of peroxidases. Thus, superoxide may also promote reduction of heme peroxidases from their ferric to ferrous forms by an indirect pathway.

The results of the present study demonstrate that reduction of ferric EPO, LPO, and MPO heme groups into their corresponding ferrous forms significantly affects their catalytic sites, differentially influencing heme iron reactivity and coordination structure for each peroxidase. A simplified model illustrating functional changes (with respect to affinity for diatomic ligands) to the heme pocket of EPO, LPO, and MPO that occur upon reduction is shown in Figure 8. The active site of ferrous EPO remains accessible to diatomic ligands such as NO and CO, rapidly generating the corresponding six-coordinate complexes. In contrast, access of diatomic ligands such as NO (*25*) and CO (this study) to ferrous MPO is significantly impaired, suggesting collapse or narrowing of the heme pocket following reduction. Finally, reduction of LPO results in formation of two spectroscopically (Figure 2B) and kinetically (Figure 7) distinguishable forms of enzyme that demonstrate differential reactivities to diatomic ligands consistent with the presence of an open and

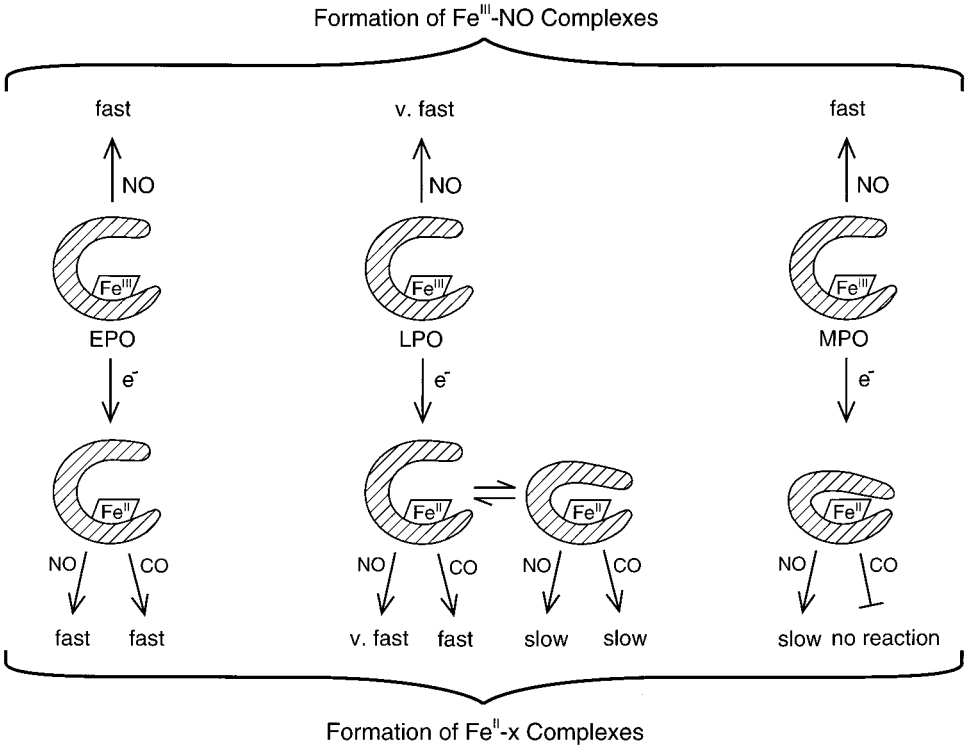

FIGURE 8: Simplified model describing the perturbations in the heme environment for EPO, LPO, and MPO that occur upon heme reduction.

a closed form (Figure 8). In Figure 8, closed forms of ferrous peroxidases (MPO and one of the LPO intermediates) are schematically illustrated as a collapse or narrowing of the heme pocket, preventing access of diatomic ligands to the distal catalytic center. Narrowing in the heme pocket geometry upon LPO−Fe(III) and MPO−Fe(III) reduction may result from significant increases in the affinity of the heme iron toward a sixth ligand provided by either a water molecule or one of the amino acids located above the heme prosthetic group (*25*, *33*, *34*, *43*). Indeed, the X-ray crystal structure of MPO−Fe(III) reveals that the imidazole ring of His^{95} is located only 5.7 Å from the heme iron (*33*, *34*, *80*). The guanidinium group of Arg^{239} and the side chain of Gln^{91} also lie close to the heme surface with minimum interatomic distances of 7.0 and 4.5 Å, respectively, to the iron atom (*33*, *34*, *80*). Thus, either steric interactions or an alteration in the potential coordination of the heme iron likely accounts for the hindered interactions of NO and CO with ferrous forms of MPO and LPO.

The presence of two different conformational states of LPO−Fe(II) has been reported in studies using rapid kinetic measurement (*56*), resonance Raman spectroscopy (*81*), and UV/vis spectroscopy (*82*). However, functional differences between the two forms have not been reported. For example, resonance Raman spectroscopy studies demonstrated that the equilibrium species display no significant differences in the character of the Fe−N(histidine) bond, and both share the same spin-state configuration (*75*). The present studies revealed that reduction of LPO−Fe(III) generates at least two spectroscopically and kinetically distinguishable species in equilibrium, which are functionally distinguishable on the basis of their rates of binding to diatomic ligands; i.e., their behavior mirrors that observed with MPO−Fe(II) (closed form) and EPO−Fe(II) (open form). Upon reduction of LPO−Fe(III) heme, an initial rapid buildup of an LPO−Fe(II) species (Figure 2) that displays a relatively open heme pocket geometry is observed, as judged by its ability to bind CO and NO at a fast rate. Approximately 50% of this transient intermediate is gradually converted into another LPO species that binds to CO at a slower rate, consistent with a conformational alteration that results in narrowing of the heme pocket. Both LPO species are populated at equilibrium and can be distinguished by their characteristic optical spectra (Figure 2) and their ability to bind CO at distinct rates (Figure 7). At equilibrium, CO binds to one of the Fe(II) forms slowly, with a second-order rate constant that is 24-fold slower than that observed with the faster form. Similarly, the second-order rate constant for the dissociation of CO from this form is also 22-fold slower than that observed with the other equilibrium form. Biphasic rates of CO binding have also been reported for Fe(II) forms of NOSs and other hemoproteins (*53*, *83*).

X-ray studies with model porphyrins indicate that Fe−CO complexes are more rigid than Fe−NO complexes and consequently occupy more space (*84*, *85*). Thus, binding of CO to a sterically restricted form of the enzyme should be more difficult than that observed for NO. Indeed, incubation of CO with MPO−Fe(II) caused little or no alteration in the Soret and visible region, as was first reported by Agner (*63*). The small changes in optical spectra in the presence of saturating concentrations of CO have been interpreted as binding of the diatomic ligand to the MPO Fe(II) moiety (*86*, *87*). However, when interpreted within the context of the dramatically decreased k_{on} and k_{off} of another (smaller) diatomic ligand, NO (Table 1), and the rates of diatomic ligand interactions with the ferric and ferrous forms of EPO and LPO, we speculate that the results are consistent with MPO heme reduction preventing CO binding altogether—

either by a conformational change that narrows the heme pocket geometry filling the space above the heme moiety or by higher binding affinity of heme iron toward a sixth ligand that prevents CO access to heme iron.

It should be noted that there is increasing evidence that hydrogen bonding and electrostatic field interactions, and not necessarily structural alterations in heme pocket geometry, play a contributory and even predominant role in ligand discrimination by hemoproteins (*88*−*92*). In the case of NO binding to Fe(III) forms of hemoproteins, NO donates an electron from the σ orbital to the heme iron. In contrast, in the case of NO binding to Fe(II), NO serves as an electron acceptor through its π orbital (*88*). Thus, a factor that may contribute to the dramatic differences in affinity noted between NO and the ferrous forms of mammalian peroxidases may be that the heme iron of MPO−Fe(II) is a worse Lewis acid than either EPO−Fe(II) or LPO−Fe(II) (the rapid binding conformer). Similar arguments can be made for a role of electronic interactions influencing CO binding to Fe(II).

Recently, we demonstrated that NO serves as a physiological substrate for members of the mammalian peroxidase superfamily (*25*, *26*). NO and H_2O_2 consumption by peroxidases follows the same mechanism but with different microscopic rate constants. We have also demonstrated that MPO may play a role in atherogenesis by conversion of LDL into a high-uptake form for macrophages, capable of promoting cholesterol deposition and foam cell formation, critical events in the atherosclerotic process (*93*−*95*). Peroxidases such as MPO, EPO, and LPO are also enriched in asthmatic airways (*96*−*99*), and we have demonstrated that EPO and MPO play a role in protein oxidative modification in asthma, a chronic inflammatory process that is reaching epidemic proportions in industrialized countries (*67*, *68*, *93*−*95*). Thus, a wealth of evidence suggests that mammalian peroxidases may play a critical role not only in host defense but also in disease processes. Obtaining a better structural and mechanistic understanding of these hemoproteins is a necessary step in the development of pharmacological interventions designed to selectively inhibit these enzymes.

ACKNOWLEDGMENT

We thank Dr. Dennis Stuehr for generous access to some of the instrumentation used for this study. We also thank Dr. Shome Mitra for reviewing the manuscript.

REFERENCES

1. Belding, M. E., Klebanoff, S. J., and Ray, C. G. (1970) *Science 16*, 195−196.
2. Kimura, S., and Ikeda-Saito, M. (1988) *Proteins: Struct., Funct., Genet. 3*, 113−120.
3. Ten, R. M., Pease, L. R., McKean, D. J., Bell, M. P., and Gleich, G. J. (1989). *J. Exp. Med. 169*, 1757−1769.
4. Ueda, T., Sakamaki, K., Kuroki, T., Yano, I., and Nagata, S. (1997) *Eur. J. Biochem. 243*, 32−41.
5. Petrides, P. E. (1998) *J. Mol. Med. 76*, 688−698.
6. Jong, E. C., Henderson, W. R., and Klebanoff, S. J. (1980) *J. Immunol. 124*, 1378−1382.
7. Jong, E. C., and Klebanoff, S. J. (1980) *J. Immunol. 124*, 1949−1953.
8. Weiss, S. J., Test, S. T., Eckmann, C. M., Roos, D., and Regiani, S. (1986) *Science 234*, 200−203.
9. Mayeno, A. N., Curran, A. J., Roberts, R. L., and Foote, C. S. (1989). *J. Biol. Chem. 264*, 5660−5668.
10. Klebanoff, S. J., Waltersdorph, A. M., and Rosen, H. (1984) *Methods Enzymol. 105*, 399−403.
11. Albrich, J. M., McCarthy, C. A., and Hurst, J. K. (1981) *Proc. Natl. Acad. Sci. U.S.A. 78*, 210−214.
12. Rosen, H., and Klebanoff, S. J. (1982) *J. Biol. Chem. 257*, 13731−13735.
13. van der Vliet, A., Eiserich, J. P., Halliwell, B., and Cross, C. E. (1997) *J. Biol. Chem. 272*, 7617−7625.
14. Eiserich, J. P., Hristova, M., Cross, C. E., Jones, A. D., Freeman, B. A., Halliwell, B., and van der Vliet, A. (1998) *Nature 391*, 393−397.
15. Weiss, S. L. (1989) *N. Engl. J. Med. 320*, 365−376.
16. Heinecke, J. W., Li, W., Daehnke, H. L., III, and Goldstein, J. A. (1993) *J. Biol. Chem. 268*, 4069−4077.
17. Hazen, S. L., Hsu, F. F., Mueller, D. M., Crowley, J. R., and Heinecke, J. W. (1996*) J. Clin. Invest. 98*, 1283−1289.
18. Hazen, S. L., d'Avignon, A., Anderson, M. M., Hsu, F. F., and Heinecke, J. W. (1998*) J. Biol. Chem. 273*, 4997−5005.
19. Kettle, A. J., and Winterbourn, C. C. (1997) *Redox Rep. 3*, 3−15.
20. Furtmuller, P. G., Burner, U., Regelsberger, G., and Obinger, C. (2000) *Biochemistry 39*, 15578−15584
21. Podrez, E. A., Abu-Soud, H. M., and Hazen, L. H. (2000) *Free Radical Biol. Med. 28*, 1717−1725.
22. Marquez, L. A., Dunford, H. B., and Van Wart, H. (1990) *J. Biol. Chem. 265*, 5666−5670.
23. Dunford, H. B. (1999) in *Heme Peroxidases*, pp 349−385, Wiley-VCH, New York.
24. Bolscher, B. G., Zoutberrg, G. R., Cuperus, R. A., and Wever, R. (1984) *Biochim. Biophys. Acta 784*, 189−191.
25. Abu-Soud, H. M., and Hazen, S. L. (2000) *J. Biol. Chem. 275*, 5425−4530.
26. Abu-Soud, H. M., and Hazen, S. L. (2000) *J. Biol. Chem. 275*, 37524−37532.
27. Kettle, A. J., Sangster, D. F., Gebicki, J. M., and Winterbourn, C. C. (1988*) Biochim. Biophys. Acta 956*, 58−62.
28. Klebanoff, S. J., and Clark, R. A. (1978) *The Neutrophil: Functions and Clinical Disorders*, pp 1−810, Elsevier Science Publisher B. V., Amsterdam.
29. Nauseef, W. M., and Malech, H. L. (1986) *Blood 67*, 1504−1507.
30. Nauseef, W. M., Cogley, M., and McCormick, S. (1996) *J. Biol. Chem. 271*, 9546−9549.
31. Dugad, L. B., La Mar, G. N., Lee, H. C., Ikeda-Saito, M., Booth, K. S., and Caughey, W. S. (1990) *J. Biol. Chem. 265*, 7173−7179.
32. Taylor, K. T., Stroble, F., Yue, K. T., Ram, P., Pohl, J., Woods, A. S., and Kinkade, J. M., Jr. (1995) *Arch. Biochem. Biophys. 316*, 635−642.
33. Zeng, J., and Fenna, R. E. (1992) *J. Mol. Biol. 226*, 185−207.
34. Davey, C. A., and Fenna, R. E. (1996) *Biochemistry 35*, 10967−10974.
35. Caulfield, J. P., Korman, G., Butterworth, A. E., Hogan, M., and David, J. R. (1980) *J. Cell Biol. 86*, 46−63.
36. Arlandson, M., Decker, T., Roongta, V. A., Bonilla, L., Mayo, K. H., MacPherson, J. C., Hazen, S. L., and Slungaard, A. (2001) *J. Biol. Chem. 276*, 215−224.
37. Dull, T. J., Uyeda, C., Strosberg, A. D., Newdwin, G., and Seilhamer, J. J. (1990*) DNA Cell Biol. 9*, 499−509.
38. Cals, M. M., Mailliart, P., Brignon, G., Anglade, P., and Dumas, B. R. (1991) *Eur. J. Biochem. 198*, 733−739.
39. Ferrari, R. P., Laurenti, E., Cecchini, P. I., Gambino, O., and Sondergaard, I. (1995) *J. Inorg. Biochem. 58*, 109−127.
40. Carlstrom, A. (1969) *Acta Chem. Scand. 23*, 185−202.
41. Reiter, B., and Perraudin, J. P. (1991) in *Peroxidases in Chemistry and Biochemistry* (Everse, K. E., and Grisham, M. B., Eds.) Vol. 1, pp 143−180, CRC Press, Boca Raton, FL.
42. Wolfson, L. M., and Sumner, S. S. (1993) *J. Food Prot. 56*, 887−892.
43. De Gioia, L., Ghibaudi, E. M., Laurenti, E., Salmona, M., and Ferrari, R. P. (1996) *J. Biol. Inorg. Chem. 1*, 476−485.
44. Palmer, R. M. J., Ferrige, A. G., and Moncada, S. (1987) *Nature 327*, 524−526.

45. Ignarro, L. J., Buga, G. M., Wood, K. S., Byrns, R. E., and Chaudhuri, G. (1987) *Proc. Natl. Acad. Sci. U.S.A. 84*, 9265−9269.
46. Wink, D. A., Osawa, Y., Darbyshire, J. F., Collins, R. J., Eshenaur, S. C., and Nims, R. W. (1993) *Arch. Biochem. Biophys. 300*, 115−123.
47. Castro, L., Rodriguez, M., and Radi, R. (1994) *J. Biol. Chem. 269*, 29409−29415.
48. Freeman, B. A., White, R. C., Paler-Martinez, A., Tarpey, M. M., and Rubbo, H. (1995) in *Nitric Oxide: Biochemistry, Molecular Biology, and Therapeutic Implications* (Ignarro, L., and Murad, F., Eds.) vol. 34 of *Advances in Pharmacology*, pp 45−69, Academic Press.
49. Abu-Soud, H. M., Wang, J., Rousseau, D. L., Fukuto, J. M., Ignarro, L. J., and Stuehr, D. J. (1995) *J. Biol. Chem. 270*, 22997−23006.
50. Hurshman, A. R., and Marletta, M. A. (1995) *Biochemistry 34*, 5627−5634.
51. Cooper, C. E. (1999) *Biochim. Biophys. Acta 1411*, 290−309.
52. Rose, E. J., and Hoffman, B. M. (1993) *J. Am. Chem. Soc. 105*, 2866−2873.
53. Abu-Soud, H. M., Wu, C., Ghosh, K. D., and Stuehr, D. J. (1998) *Biochemistry 37*, 3777−3786.
54. Sharma, V. S., Taylor, T. G., and Gardiner, R. (1987) *Biochemistry 26*, 3837−3843.
55. Radi, R. (1996) *Chem. Res. Toxicol. 9*, 828−835.
56. Lange, R., Heiber-Langer, I., Bonfils, C., Fabre, I., Negishi, M., and Balny, C. (1994) *Biophys. J. 66*, 89−98.
57. Wu, W., Chen, Y., and Hazen, S. L. (1999) *J. Biol. Chem. 274*, 25933−25944.
58. Rakita, R. M., Michel, B. R., and Rosen, H. (1990) *Biochemistry 29*, 1075−1080.
59. Wever, R., Plat, H., and Hamers, M. N. (1981) *FEBS Lett. 123*, 327−331.
60. Agner, K. (1963) *Acta Chem. Scand. 17*, S332−S338.
61. Carlson, M. G., Peterson, C. G., and Venge, P. (1985) *J. Immunol. 134*, 1875−1879.
62. Thayer, J. R., and Huffaker, R. C. (1980) *Anal. Biochem. 102*, 110−119.
63. Agner, K. (1941) *Acta Physiol. Scand. 2*, 5-60.
64. Brennan, M.-L., Anderson, M. M., Shih, D. M., Qu, X.-D., Mehta, A. C., Lim, L. L., Shi, W., Jacob, J. S., Cowley, J. R., Hazen, S. L., Wang, X., Heinecke, J. W., and Lusis, A. J. (2001) *J. Clin. Invest. 107*, 419−430.
65. Nauseef, W. M. (1999) *J. Lab. Clin. Med. 134*, 215−221.
66. Klebanoff, S. J. (1999) *Proc. Assoc. Am. Physicians 111*, 383−389.
67. MacPherson, J. C., Comhair, S. A., Erzurum, S. C., Klein, D. F., Lipscomb, M. F., Kavuru, M. S., Samoszuk, M. K., and Hazen, S. L. (2001) *J. Immunol. 166*, 5763−5772.
68. Wu, W., Samoszuk, M. K, Comhair, S. A., Thomassen, M. J., Farver, C. F, Dweik, R. A., Kavuru, M. S., Erzurum, S. C., and Hazen, S. L. (2000) *J. Clin. Invest. 105*, 1455−1463.
69. Sugiyama, S., Okada, Y., Sukhova, G. K., Virmani, R., Heinecke, J. W., and Libby, P. (2001*) Am. J. Pathol. 158*, 879−891.
70. Stone, J. R., and Marletta, M. A. (1994) *Biochemistry 33*, 5636−5640.
71. Gerzer, R., Bohme, E., Hofmann, F., and Schultz, G. (1981) *FEBS Lett. 132*, 71−74.
72. Tsai, A., Wei, C., and Kulmacz, R. J. (1994) *Arch. Biochem. Biophys. 313*, 367−372.
73. Ikeda-Saito, M. (1987) *Biochemistry 26*, 4344−4349.
74. Salmaso, B. L. N., Puppels, G. J., Caspers, P. J., Floris, R., Wever, R., and Greve, J. (1994) *Biophys. J. 67*, 436−446.
75. Manthey, J. A., Boldt, N. J., Bocian, D. F., and Chan, S. I. (1986) *J. Biol. Chem. 261*, 6734−6741.
76. Sibbett, S. S., Klebanoff, S. J., and Hurst, J. K. (1985) *FEBS Lett. 189*, 271−275
77. Lukat, G. S., Rodgers, K. R., and Goff, H. M. (1987) *Biochemistry 26*, 6927−6932.
78. Abu-Soud, H. M., Ichimori, K., Presta, A., and Stuehr, D. J. (2000) *J. Biol. Chem. 275*, 17349−17357.
79. Sharma, V. S., Isaacson, R. A., John, M. E., Waterman, M. R., and Chevion, M. (1983) *Biochemistry 22*, 3897−3902.
80. Fiedler, T. J., Davey, C. A., and Fenna, R. E. (2000) *J. Biol. Chem. 275*, 11964−11971.
81. Hu, S., Treat, R. W., and Kincaid, J. R. (1993) *Biochemistry 32*, 10125−10130.
82. Sharonov, Y. A. (1995) *FEBS Lett. 377*, 512−514.
83. Scheele, J. S., Kharitonov, V. G., Martasek, P., Roman, L. J., Sharma, V. S., Masters, B. S. S., and Magde, D. (1997) *J. Biol. Chem. 272*, 12523−12528.
84. Hoard, J. L. (1975) in *Porphyrins and Metalloporphyrins* (Smith, K. M., Ed.) pp 356−358, Elsevier, New York.
85. Peng, S., and Ibers, J. (1976) *J. Am. Chem. Soc. 98*, 8032−8036.
86. Odajima, T., and Yamazaki, I. (1970) *Biochim. Biophys. Acta 206*, 71−77.
87. Edwards, S. W., and Lloyed, D. (1987) *Biosci. Rep. 7*, 193−199.
88. Brucker, E. A., Olson, J. S., Ikeda-Saito, M., and Phillips, G. N. (1998) *Proteins: Struct., Funct., Genet. 30*, 352−356.
89. Decatur, S. M., Franzen, S., DePillis, G. D., Dyer, R. B., Woodruff, W. H., and Boxer, S. G. (1996) *Biochemistry 35*, 4939−4944.
90. Park, K. D., Guo, K. M., Adebodun, F., Chiu, M. L., Sligar, S. G., and Oldfield, E. (1991) *Biochemistry 30*, 2333−2347.
91. Eich, R. F., Li, T., Lemon, D. D., Doherty, D. H., Curry, S. R., Aitken, J. F., Mathews, A. J., Johnson, K. A., Smith, R. D., Phillips, G. N., and Olson, J. S. (1996) *Biochemistry 35*, 6976−6983.
92. Olson, J. S., and Phillips, G. N. (1996) *J. Biol. Chem. 271*, 17593−17596.
93. Podrez, E. A., Febbraio, M., Sheibani, N., Schmitt, D., Silverstein, R. L., Hajjar, D. P., Cohen, P. A., Frazier, W. A., Hoff, H. F., and Hazen, S. L. (2000) *J. Clin. Invest. 105*, 1095−1108.
94. Podrez, E. A., Schmitt, D., Hoff, H. F., and Hazen, S. L. (1999) *J. Clin. Invest. 103*, 1547−1560.
95. Mitra, S. N., Slungaard, A., and Hazen, S. L. (2000) *Redox Rep. 5*, 215−224.
96. Holt, P. G., Macaubas, C., Stumbles, P. A., and Sly, P. D. (1999) *Nature 402*, B12−17.
97. Gleich, G. J., Ottesen, E. A., Leiferman, K. M., and Ackerman, S. J. (1989) *Int. Arch. Allergy Appl. Immunol. 88*, 59−62.
98. Matthias, S., Holderby, M., Forteza, R., Abraham, W. M., Wanner, A., and Conner, G. E. (1977) *Am. J. Respir. Cell Mol. Biol. 17*, 97−105.
99. Rothenberg, M. E. (1998) *N. Engl. J. Med. 338*, 1592−1600.

BI010478V